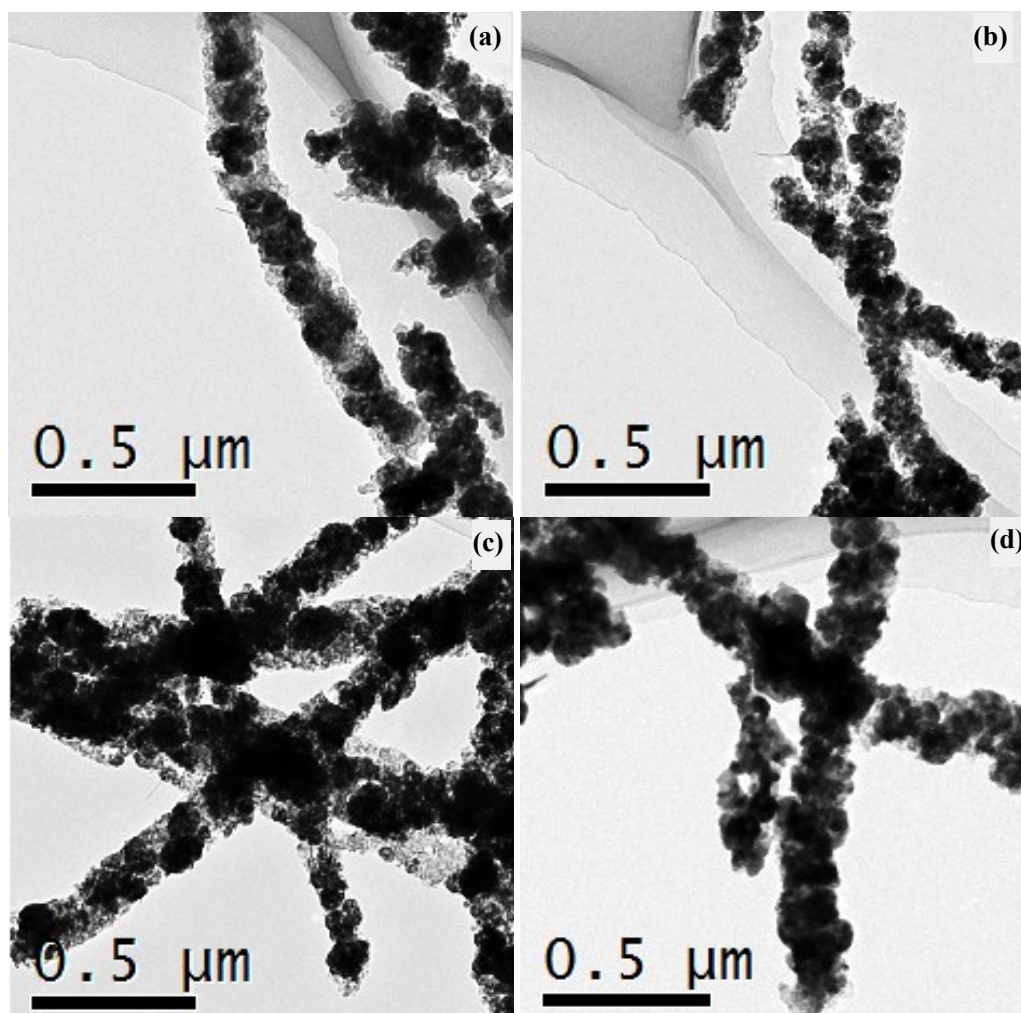


Supporting Information

Tuning electrical conductivity of amorphous carbon-reduced graphene oxide wrapped-Co₃O₄ ternary nanofibers for highly-sensitive chemical sensors

Qiuxia Feng, Yamei Zeng, Pengcheng Xu, Shiwei Lin, Chao Feng, Xiaogan Li* and Jing Wang*



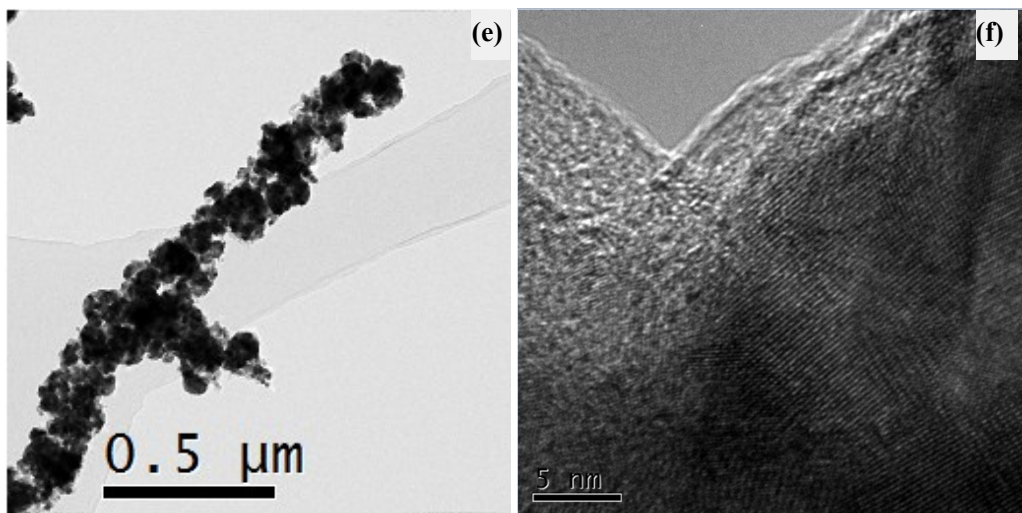


Figure S1. Morphologies of the final samples of S1 (a), S2 (b), S3 (c), S4(d), S5(e) and (f) carbon layer on some part of Co_3O_4 crystal surfaces of S6.

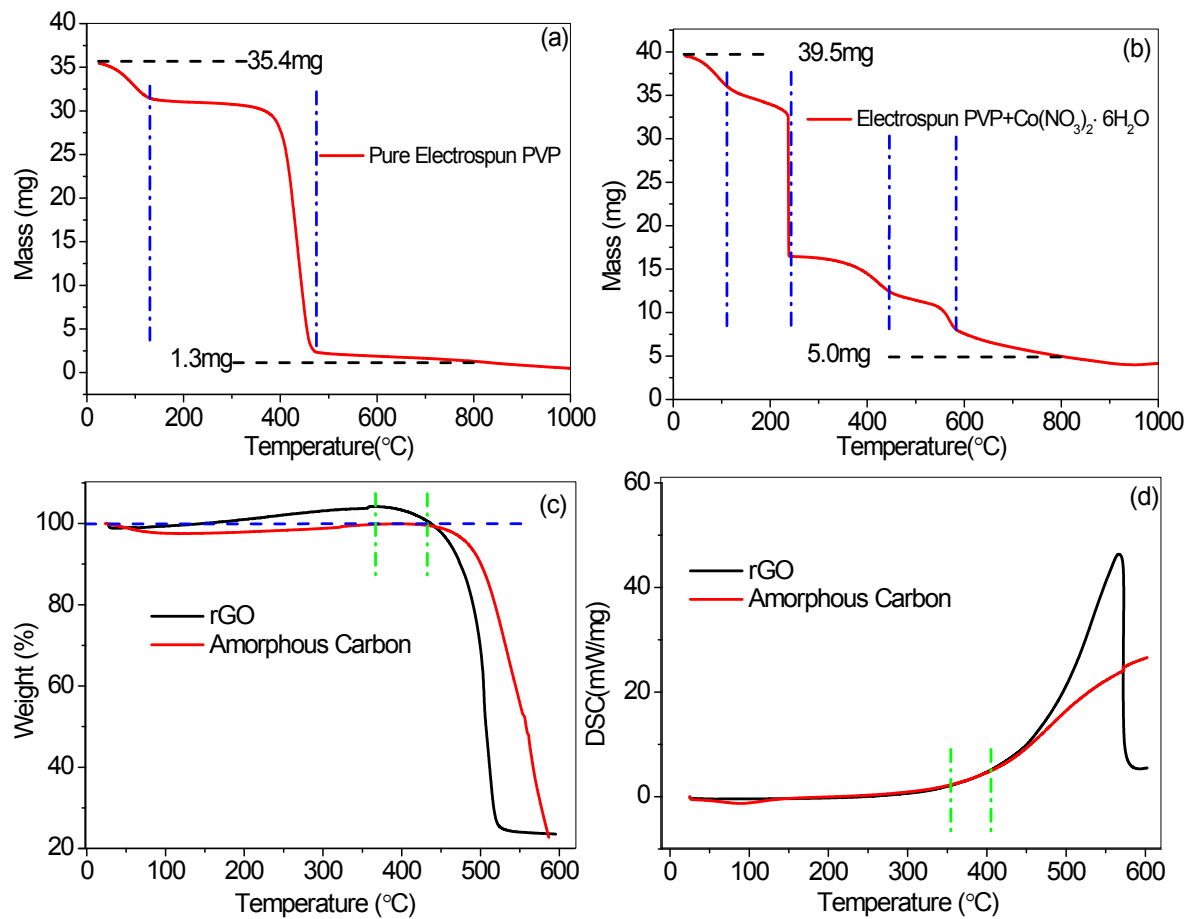


Figure S2. The TGA of precursor nanofibers of (a) pure PVP, (b) PVP + cobalt salts under nitrogen and (c) rGO and amorphous carbon under air and the DSC of (d) rGO and amorphous carbon under air.

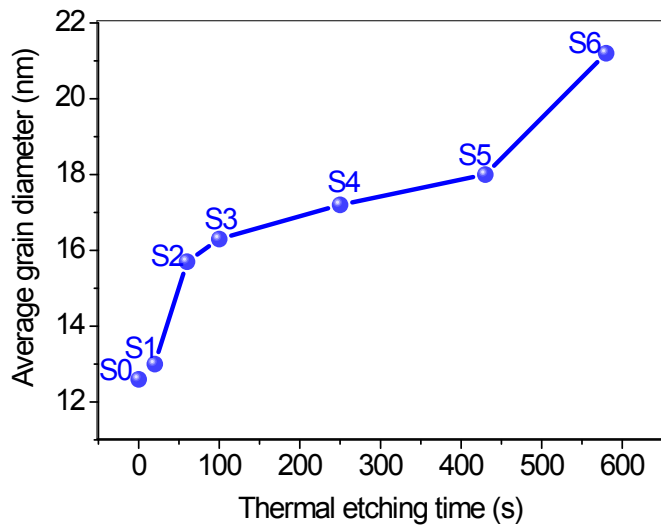
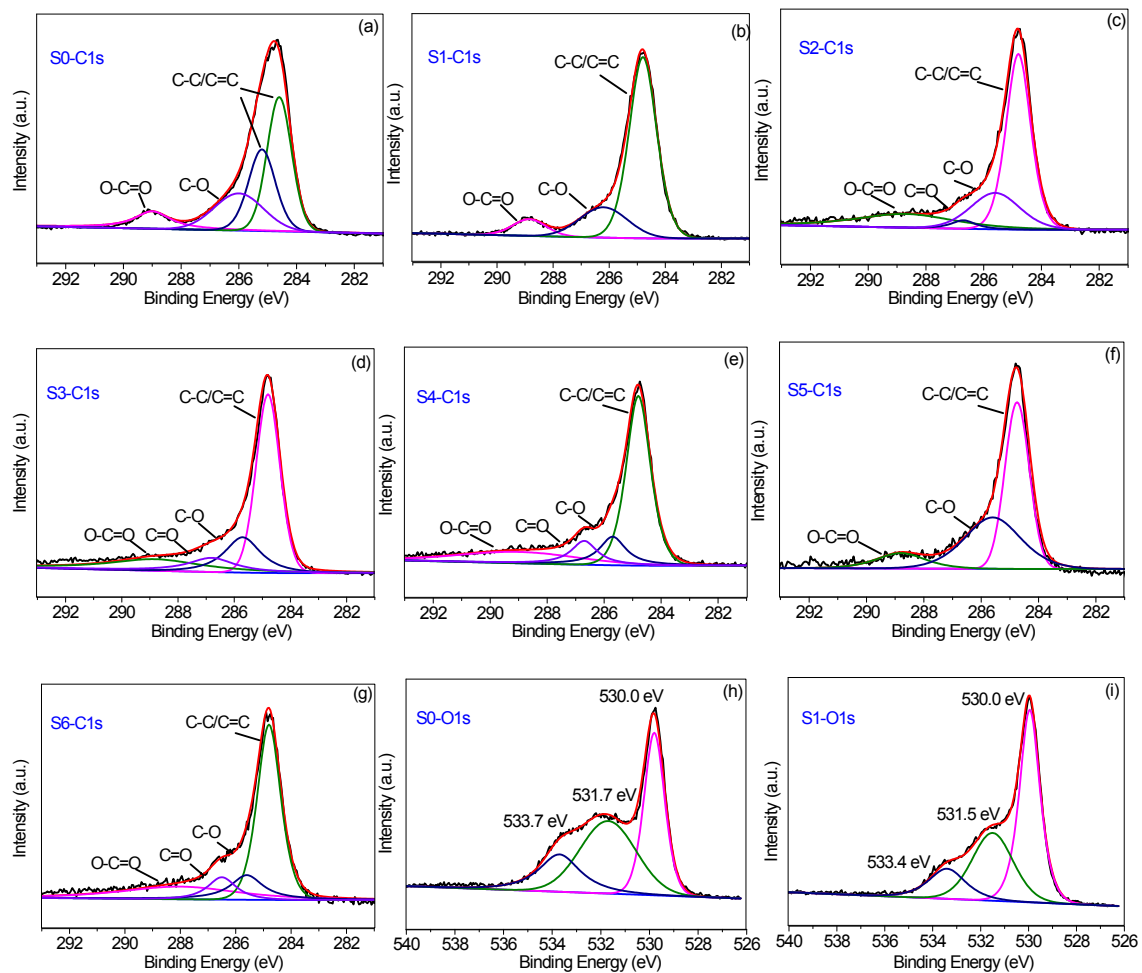


Figure S3. Correlation between the average crystal size of Co_3O_4 and the thermal etching time.



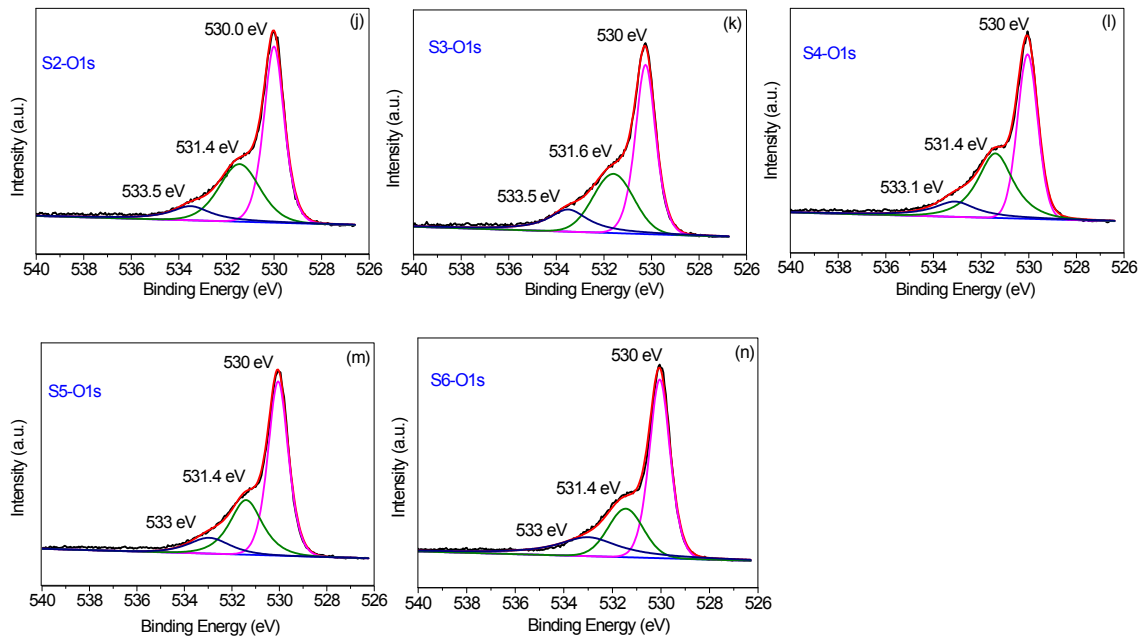


Figure S4. (a-g) Peak fittings for C 1s pattern and (h-n) Peak fittings for O 1s pattern of samples

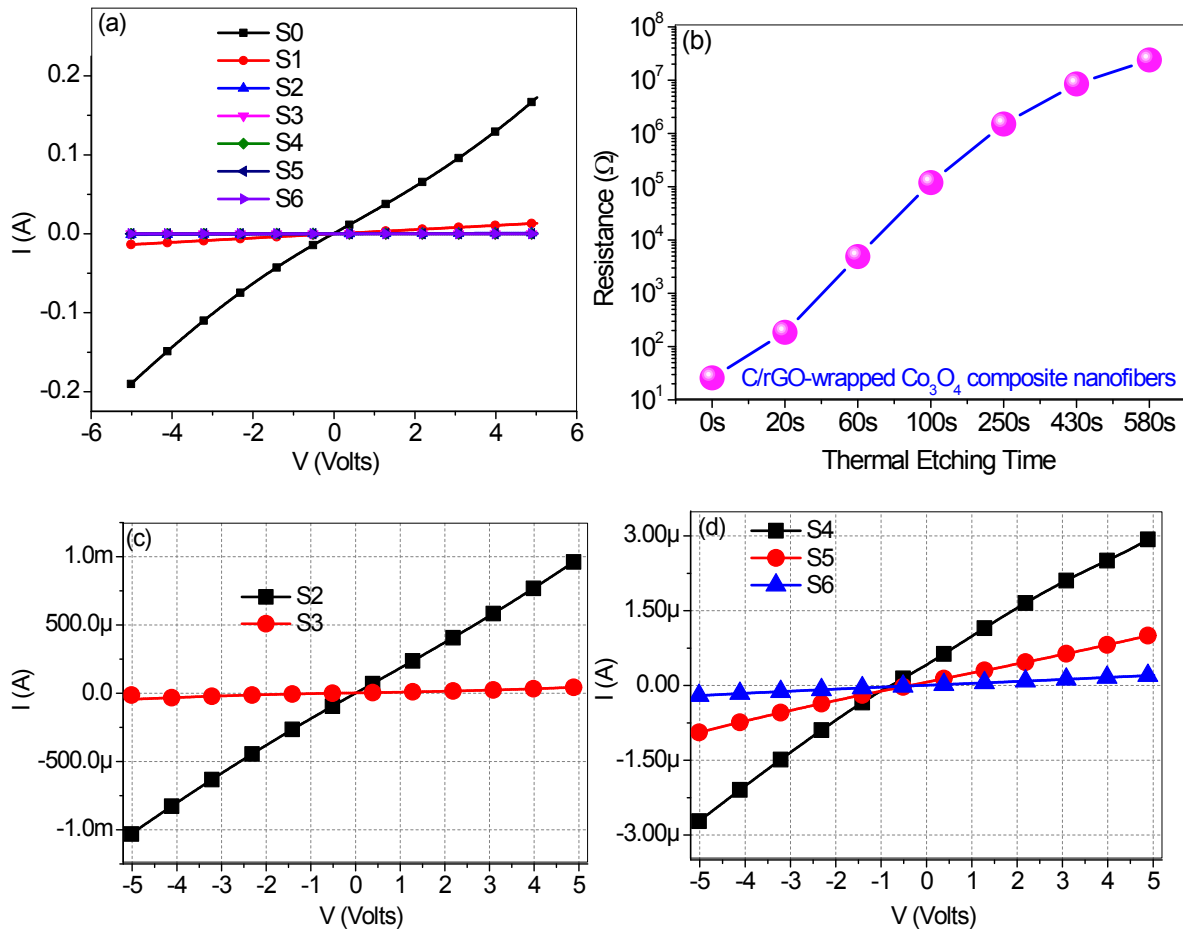


Figure S5. The I-V polarization curves of (a) S0-S6, (b) the calculation of resistance with different thermal etching time, (c) S2-S3 and (d) S4-S6.

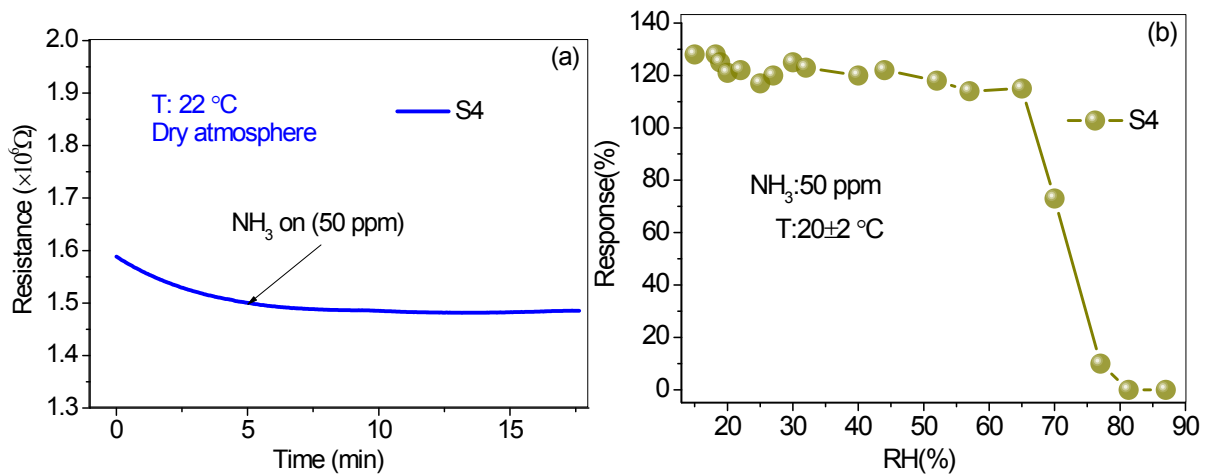


Figure S6. The response of the S4 based sensor to NH_3 of 50 ppm in (a) dry air and (b) humid air with the varied relative humidity at room temperature.

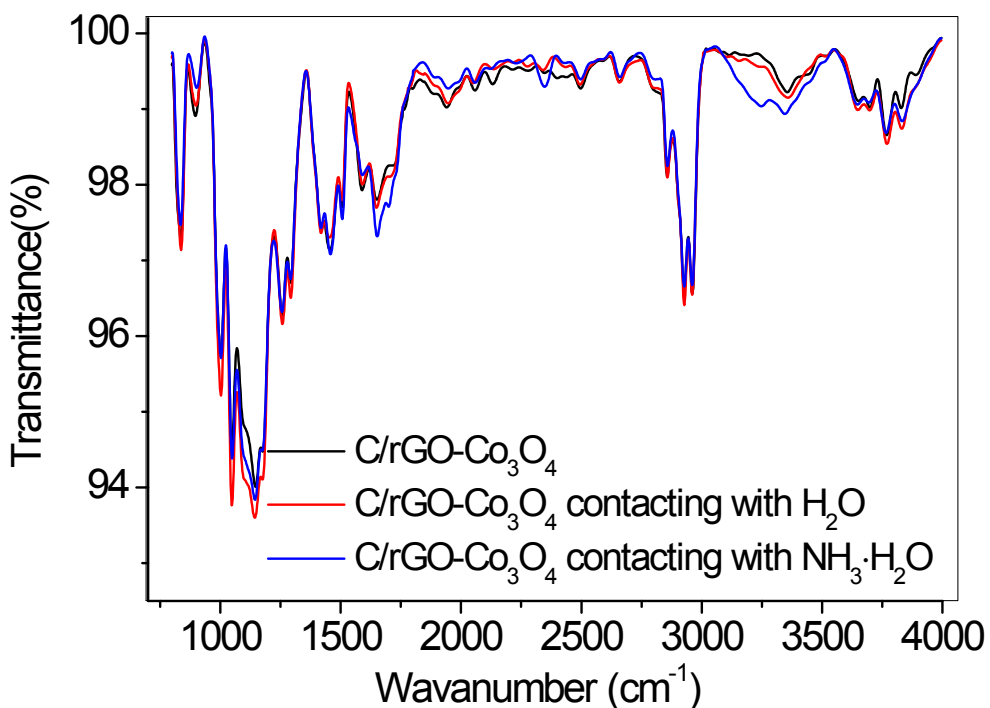


Figure S7. The in-situ FTIR patterns of S4 within the wavenumber range from 800 to 4000 cm^{-1} .

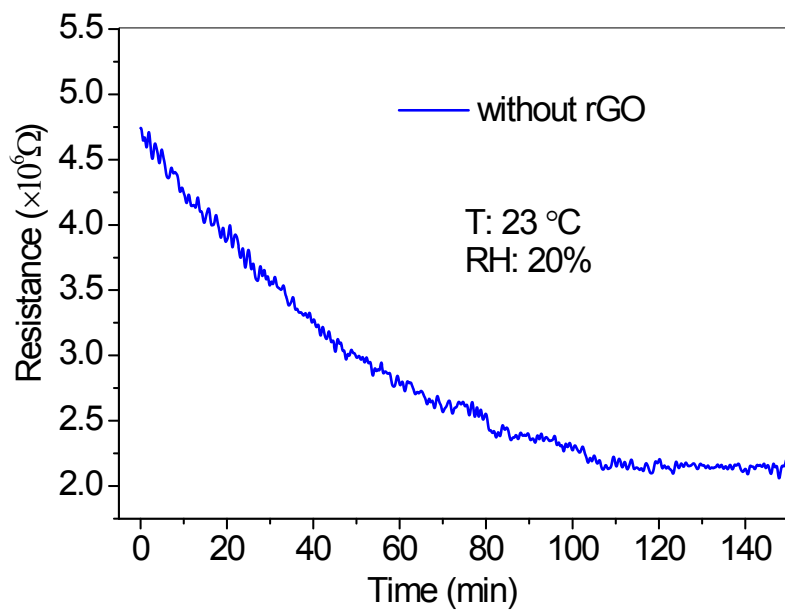


Figure S8. The stabilization process of the resistance of sensor without rGO before sensing measurement.

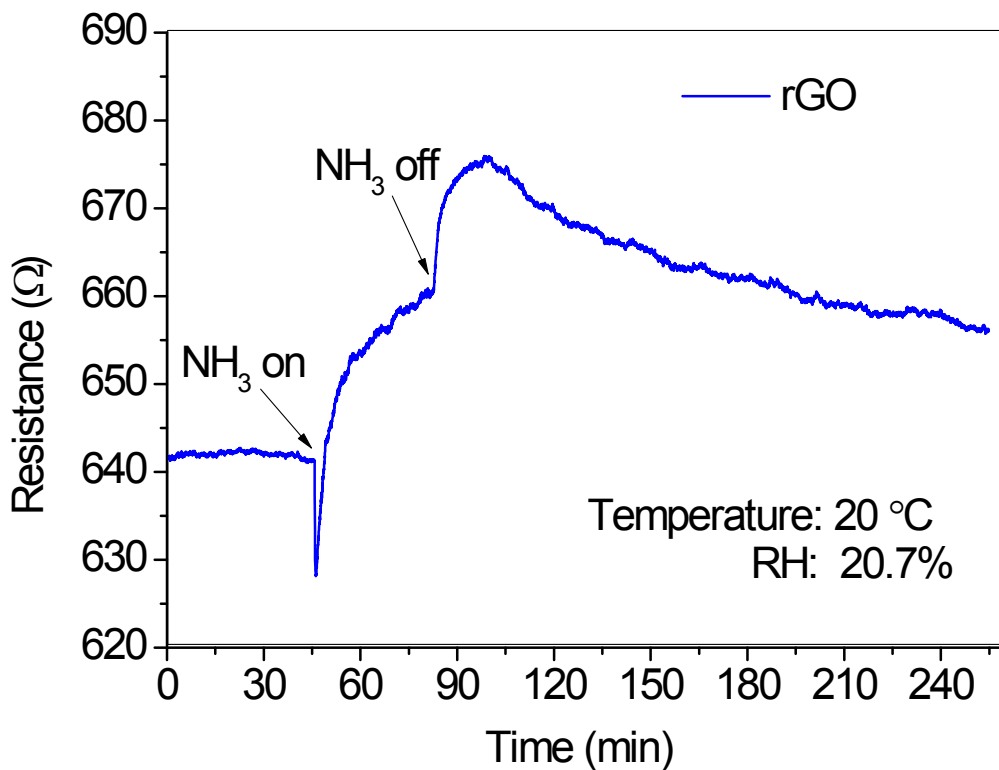


Figure S9. Response of the sensor based on rGO to NH₃ of 50 ppm at room temperature

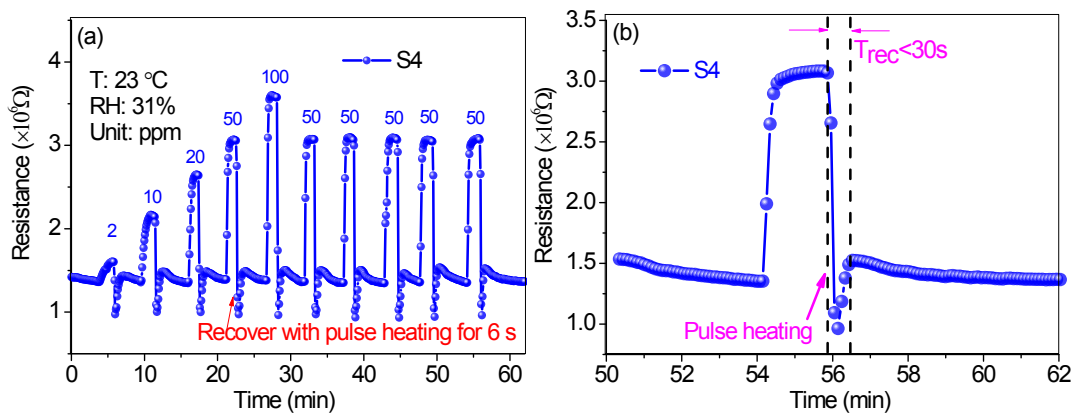


Figure S10. (a) Response to NH_3 of 1-100 ppm, the repeatability of response to NH_3 of 50 ppm and recovery with pulse heating for 6 s and (b) magnification of test for 50 ppm (the last time) in (a).

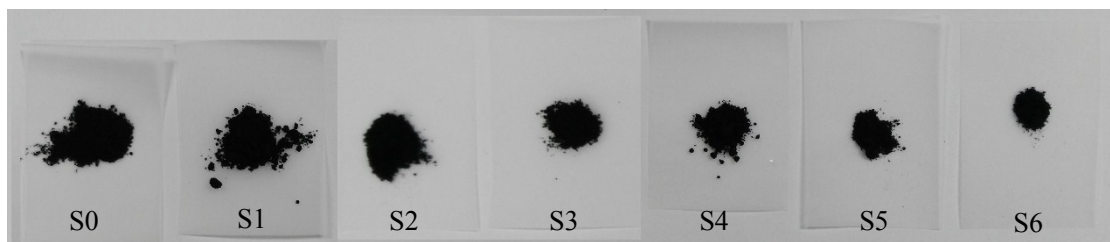


Figure S11. The photographs of S0, S1, S2, S3, S4, S5 and S6.